COMMUTATION INTERACTION ON THE OPERATION OF A 12/8 THREE PHASE SWITCHED RELUCTANCE MOTOR

M. A. Abdulatif, M. M. Khater, S. M. R. Tahoun, M. M. El-Shanawany and S. A. Hassan

Department of Electrical Engineering, Faculty of Engineering, Menoufiya University
Shebin El-Kom, EGYPT.

ABSTRACT

The conventional pair-pole per phase switched reluctance motors are now well established. This paper introduces an analytical and experimental study for a 12/8 as a different motor configuration with four poles per phase. Throughout the present study a laboratory prototype for the motor along with its electronic power converter, is built and experimentally tested to evaluate motor's steady state performance. The effect of commutation ratio on the motor performance is investigated, and an optimum range is devised to maximize the developed torque. A mathematical model is developed for the motor to predict its performance. Both computed and experimental test results are found to be in good agreement.

Keywords: Four-pole/Phase Switched Reluctance Motor, Commutation ratio.

INTRODUCTION

Switched reluctance motor (SRM) is one of the simplest known electric motors. Its development has been initiated and continued during the last two decades along with the great and rapid advances in the field of power electronics and computer systems.

SRM consists of a doubly salient structure with simple concentrated windings on its stationary member while there are no windings of any type on the rotor. In general, the windings on each two diametrically opposite stator poles are connected in series to form a phase. Torque is produced by the tendency of rotor poles to align with the stator poles of the excited phase. Since the produced torque is independent of the direction of excitation current, a simple uni-directional electronic power converter is sufficient for motor excitation. Recent research studies are mainly directed to the development of new motor configurations. Some of such studies are found in the literature and summarized here.

A switched reluctance motor with multi-tooth per pole was introduced by Finch *et al* .[1], in which better motor performance has been obtained at low speed. At such low speed of operation the frequency of flux reversals is low and core losses are within accepted level. Axial air gap configuration was introduced in Reference 2 with only two phases. Since self-starting is only possible for at least three phase motor, the author of that paper proposed the stepped air gap for the motor to be self started. SRM is often manufactured as a three or four phase motor, however, some researches introduced five and seven phase SRM configurations [3,4] for low speed operation. In these designs the winding interconnections are arranged in such a way to obtain short flux loops to reduce the core losses. Another motor configuration was introduced in which the motor winding combined between short flux path and full flux path [5]. Such combination was proposed to get better energy circulation and to utilize the energy stored in the magnetic field for torque production. A Lovatt

and Stephenson introduced four-pole per phase SRM [6] and compared with the conventional two-pole per phase motor from the point view of flux linkage and static torque, for the same thermal limitation. Steady-state characteristics of this configuration was not discussed, it still deserves more investigation.

Conventional 3-phase SRM usually consists of 6/4 stator/rotor pole combination as shown in Figure 1-a. Such motor configuration has only two pionts of pole alignment, at a time, which results-in long flux-linkage path and lacks the distribution of tangential forces around the rotor periphery.

This pole arrangement contributes a noticeable acoustic noise and a high level of torque pulsations.

This paper introduces an analytical and experimental study for the steady-state characteristics of a four-pole per phase SRM (4PSRM). The proposed motor configuration overcomes the mentioned drawbacks of the conventional one. During the present study, a laboratory prototype 4PSRM has been built and investigated. The motor steady state performance has been experimentally tested and analyzed. The relationship between the commutation ratio(CR) and motor performance has also been studied analytically and experimentally. Throughout the present study, a range for optimum commutation ratio has been devised to maximize the developed torque. Good agreement is found between the experimental and the computed results.

SYSTEM DESCRIPTION AND EXPERIMENTAL TEST RIG

The prototype of the proposed four poles per phase switched reluctance motor (4PSRM) has been assembled using a stamped stator of 36 slots, 1/3HP, single phase induction motor. One tooth has been removed from each three teeth of the used stator to create a twelve salient-pole configuration. The stator has been wound with twelve concentrated coils, where each two diametrically opposite coils are connected in series to form a branch. Each two perpendicular branches are connected in parallel to form the winding of one phase. This winding arrangement results-in four poles per phase which splits the forces up evenly around the rotor periphery and shortens the flux-linkage path. The proposed winding arrangement reduces the noise level and improves the motor performance.

An 8-pole steel laminated rotor has been designed and built for the proposed motor. The number of rotor poles has been chosen to ensure that, there is always a single magnetic flux path of minimum reluctance for each pole-pair. The motor assembly is shown in Figure 1-b in which the rotor is aligned to phase A. The motor data are given in the Appendix. An electromagnetic brake is coupled with the motor for mechanical loading.

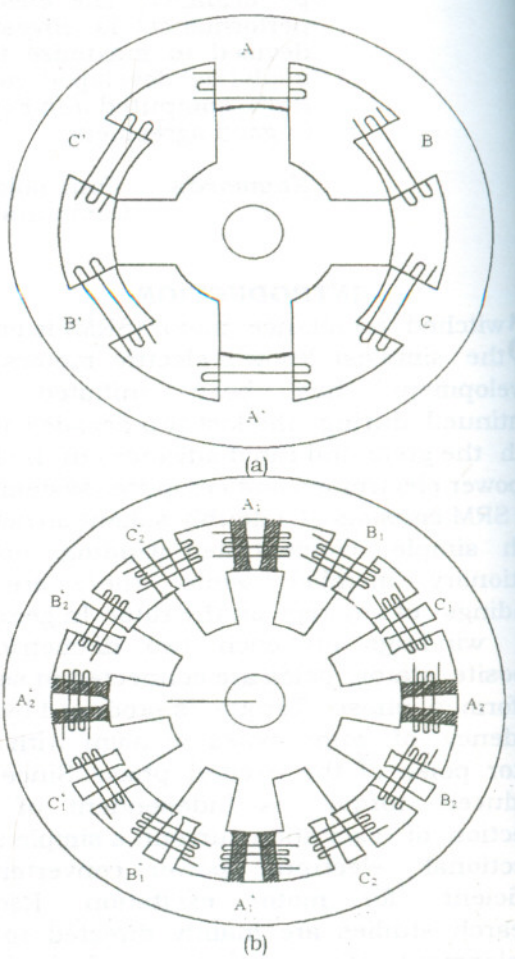

Figure 1 A cross section (a) of a conventional SRM and in the proposed 4PSRM

A shaft encoder has been designed and built for the system. This encoder consists of three U-type fixed opto-couplers, which are interrupted by a thin slotted disk mounted to the motor shaft. The encoder output signals determine both the phase excitation sequence and pulse-width. Many slotted-disks with different mark-space ratios has been prepared to test the motor performance at different commutation ratios. The encoder output signals are used to drive the electronic power converter through an interface and gate drive electronic circuits.

A six-switch asymmetric electronic power converter using six power MOSFETs has been built for the motor. The power converter circuit is shown in Figure 2. The operation sequence of each phase consists of two successive stages. During the first stage both the upper and lower MOSFETs are turned-on simultaneously to allow the phase current to be increased. In the second stage the MOSFETs are turned-off while the diodes take-over the phase current until it is extinguished. A schematic diagram for the complete experimental system is shown in Figure 3.

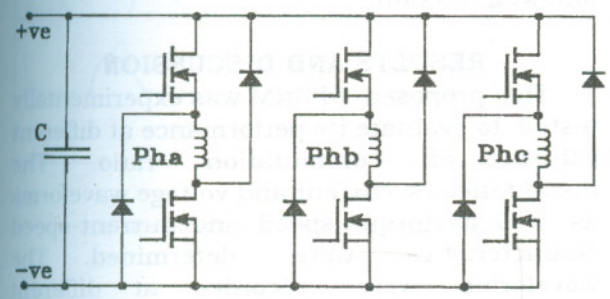

Figure 2 **The power converter circuit.**

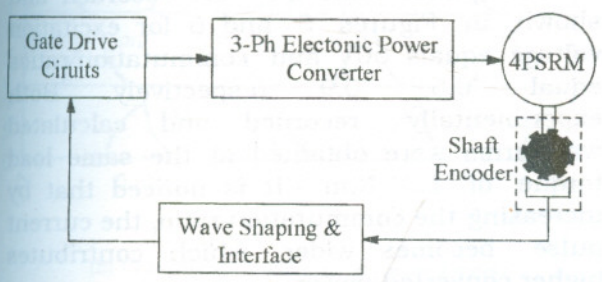

Figure 3 A schematic diagram for the experimental system.

MATHEMATICAL ANALYSIS

The motor performance is theoretically determined using a family of flux linkage-current characteristics $\psi(\theta,i)$ at different rotor positions. The method given in Reference 7 has been applied to the present motor configuration to obtain the aligned and the unaligned $\psi(\theta,i)$ curves. Since there are two parallel circuits per phase, the phase current and consequently the total MMF are twice those calculated for each circuit. A family of the $\psi(\theta,i)$ curves are generated at discrete rotor positions using the following equation[8]:

$$\psi(\theta,i) = L_u . i + \frac{\psi_a(i) - L_u . i}{2}[1 - \cos(N_r\theta)] \qquad (1)$$

where L_u is the minimum (unaligned) phase inductance, $\psi_a(i)$ represents the aligned flux linkage current curve, N_r is the number of the rotor poles, θ is the rotor position angle and i represents the phase current. These curves are rearranged and stored as a look-up table in the form of $i(\theta,\psi)$. Another important look-up table is formed from these curves which are the torque curves $T(\theta,i)$. These curves are obtained by numerical differentiation of the phase co-energy $W(\theta,i)$ relative to the rotor displacement:

$$T(\theta,i) = \frac{\partial W(\theta,i)}{\partial\theta} \qquad (2)$$

The phase co-energy is calculated by numerical integration of the $\psi(\theta,i)$ with respect to phase current:

$$W(\theta,i) = \int_0^i \psi(\theta,i)di \qquad (3)$$

To calculate the current, torque waveforms and the steady state characteristics of the motor, the circuit differential equations of all phases have to be integrated simultaneously. Since the mutual coupling between phases is too small to be considered [5]. The voltage equations are written in the form:

$$\frac{d\psi_k(\theta_k, i_k)}{dt} = \pm V_k - Ri_k \qquad (4)$$

$$\theta = \omega t$$

where R is the phase resistance, V_k is the dc applied phase voltage, k=1,2, ...,q where q is the number of phases and ω is the angular speed [9].

and

$$\theta_k = \theta_1 + (k-1)\,\varepsilon \qquad (5)$$

where ε is the step angle or the angular displacement between adjacent phases, and is given by:

$$\varepsilon = \frac{2\pi}{qN_r} \qquad (6)$$

The applied voltage on each phase is determined according to:

$$V_k = +E \text{ for } \theta_{on} \le \theta_k \le \theta_{off}$$
$$= -E \quad \theta_{off} \le \theta_k \le \theta_{ext} \qquad (7)$$
$$= 0 \quad \theta_k > \theta_{ext}$$

where E is the dc supply voltage, θ_{on} is the turn-on angle, θ_{off} is the turn-off angle, and θ_{ext} is current extinction angle.

The positive voltage is applied to each phase for a period equals to the difference between θ_{off} and θ_{on}. It is better to express this period with commutation ratio (CR) which is defined as the ratio of the angle over which the phase voltage is positive to half of the rotor pole pitch angle, or:

$$CR = \frac{\theta_c}{\tau/2} \qquad (8)$$

where $\tau = 2\pi / N_r$ is the rotor pole pitch, θ_c is the conduction angle, equals to the difference between the turn-off and the turn-on angles.

Figure 4 illustrates a schematic diagram for phase inductance and current pulse at certain commutation ratio. The relative positions for the rotor and stator poles are shown on the top of the same figure. The current pulse width can be made wider or narrower by changing the commutation ratio. This change is implemented experimentally using different slotted disks, for the shaft encoder, with different mark-space ratios.

Numerical integration is applied to Equation 4 to obtain the instantaneous phase current and torque. The look-up tables of both current and torque are used to update the current and torque values after each integration step.

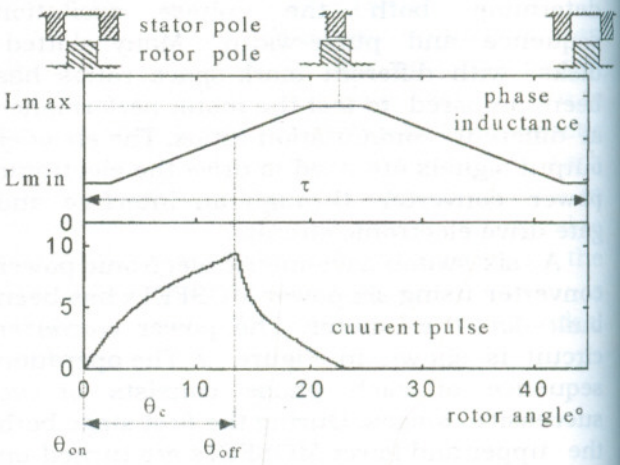

Figure 4 Phase current relative to phase inductance and poles adjustment

This mathematical model is programmed using MATLAB based on the motor dimensions as an input data. The obtained results are introduced and discussed in the following section.

RESULTS AND DISCUSSION

The proposed 4PSRM was experimentally tested to evaluate its performance at different values of commutation ratio. The instantaneous current and voltage waveforms as well as torque-speed and current-speed characteristics were determined. The waveforms were recorded at different commutation ratios ranges from 0.6 to 0.9. A sample of these results is given below.

The phase currents are recorded and shown in Figures 5 and 6 for excitation voltage equals 60V and commutation ratios equal 0.6, 0.9 respectively. Both experimentally recorded and calculated waveforms were obtained at the same load torque of 1.0 N.m. It is noticed that by increasing the commutation ratio, the current pulse becomes wider, which contributes higher converted power.

The dc-link current and the phase current as determined theoretically along with corresponding experimental values are shown in Figures 7 and 8. when the motor is fed by 60V at commutation ratios equal 0.6, 0.9 respectively. It is observed that the phase current is unidirectional while the dc link current alternates between positive and negative according to the phase switching process. The slight irregularity of the experimentally recorded dc-link current waveform is due to a little space irregularity of the corresponding phase position sensors. The relative positions of stator and rotor poles are shown on the top of the computed waveforms for both unaligned and aligned positions. It should be noted that at CR=0.9 the current pulses are too long which necessarily extend to the negative sloped inductance periods. These long current pulses results in some negative torque.

(a) Recorded phase current waveforms

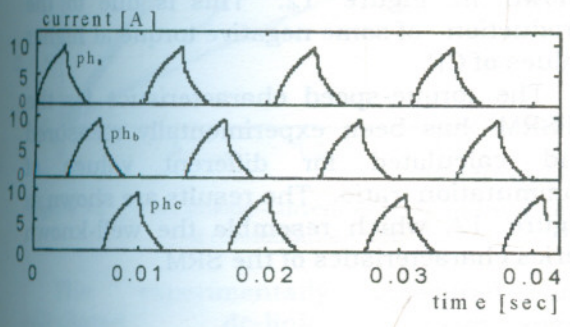

(b) Computed phase current waveforms

Figure 5 Current waveforms of the 4PSRM at speed =730 rpm, supply voltage=60V, and CR=0.6

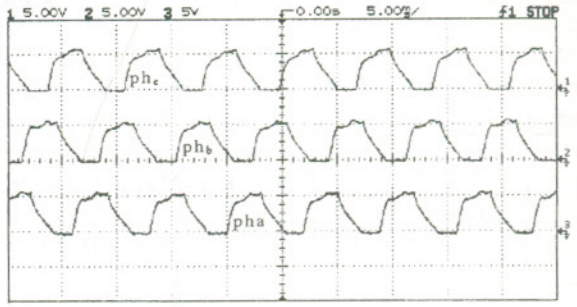

(a) Recorded phase current waveforms

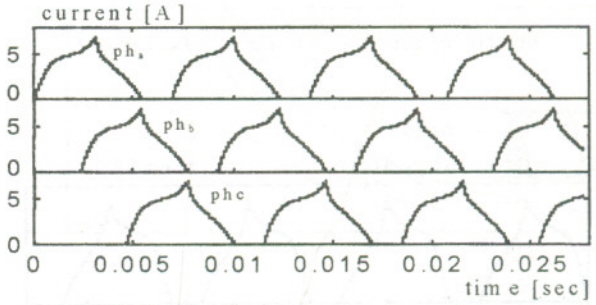

(b) Computed phase current waveforms

Figure 6 Current waveforms of the 4PSRM at speed=1085 rpm, supply voltage=60V, and CR=0.9

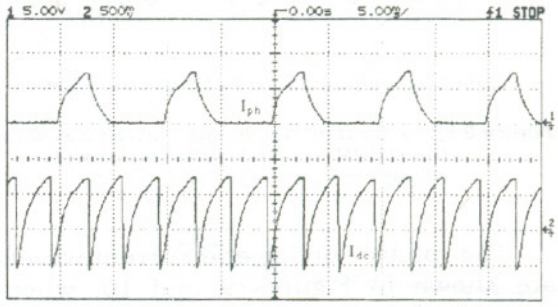

(a) The recorded waveforms

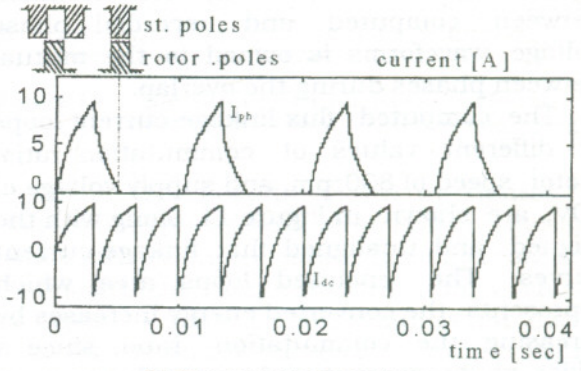

(b) The computed waveforms

Figure 7 Phase current and dc link current waveforms of the 4PSRM at speed=730 rpm, supply voltage=60V, and CR=0.6

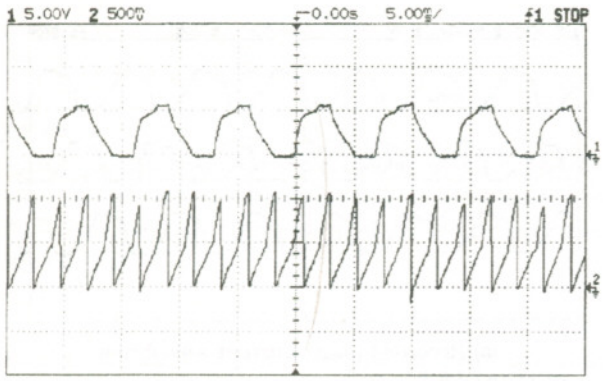

(a) The recorded waveforms at 60V, CR=0.9

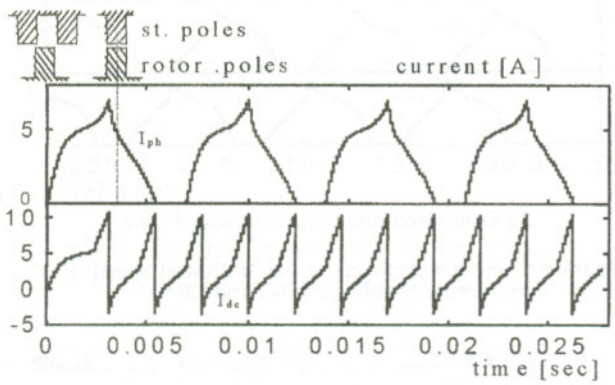

(b) The computed waveforms at 60V, CR=0.9

Figure 8 Phase current and dc link current waveforms of the 4PSRM at speed=1085 rpm, supply voltage=60V, and CR=0.9

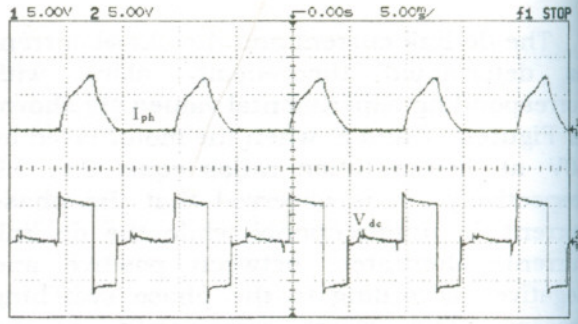

(a) The recorded waveformes

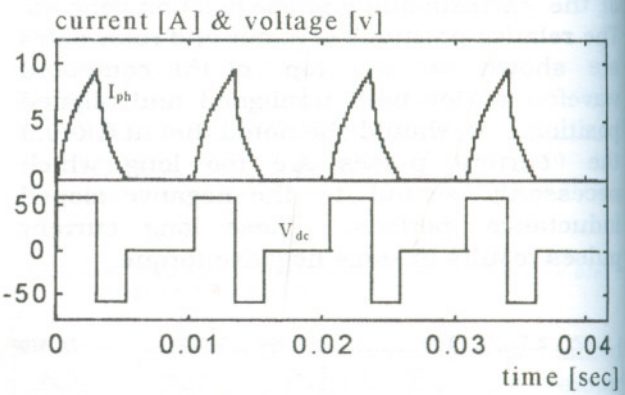

(b) The computed waveformes

Figure 9 Phase current and voltage waveforms at at speed=730 rpm, supply voltage=60V, and CR=0.6

The phase voltage and current waveforms are shown in Figures 9 and 10, when the motor is fed by 60V at commutation ratios equal 0.6, 0.9 respectively. The deviation between computed and recorded phase voltage waveforms is owned to the mutual between phases during the overlap.

The computed flux linkage-current loops at different values of commutation ratio, motor speed of 800rpm, and supply voltage of 60V, are shown in Figure 11. along with the aligned and unaligned flux linkage-current curves. The enclosed loops area which represents the converted energy increases by inreasing the commutation ratio, since a wider phase current pulse contributes more converted power. This enclosed areas are important to predict motor developed torque.

Although, the converted co-energy is increased by increasing the commutation ratio, the developed torque will decrease if commutation ratio exceeds a certain value as shown in Figure 12. This is due to the production of some negative torque at higher values of CR.

The torque-speed characteristics for the 4PSRM has been experimentally measured and calculated for different values of commutation ratio. The results are shown in Figure 12, which resemble the well-known series characteristics of the SRM.

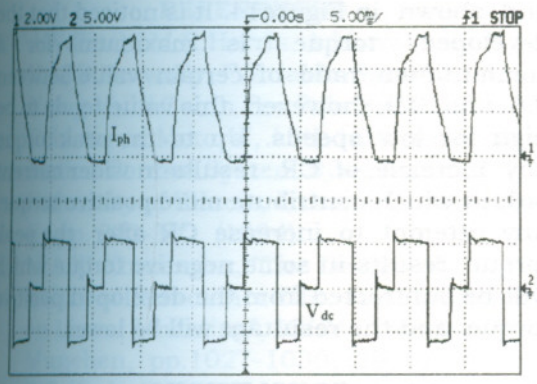

(a) The recorded waveformes

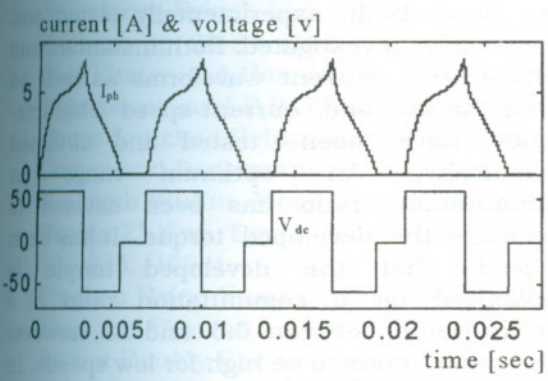

(b)The computed waveformes

Figure 10 Phase current and voltage waveforms at at speed=1085 rpm, supply voltage=60V, and CR=0.9

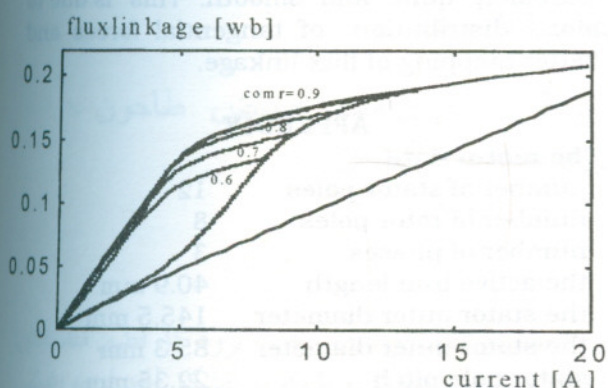

Figure 11 Flux linkage-current loops at different values of commutation ratio

The experimentally measured and calculated dc-link current-speed characteristics of the 4PSRM are shown in Figure 13. at different values of CR for 60V supply voltage. As it is shown in Figure 10, the dc link current has increased by increasing the value of CR. There is some deviation between the measured and the computed current values at low speed, because the winding current is much higher than its rating which resulted in an excessive temperature rise.

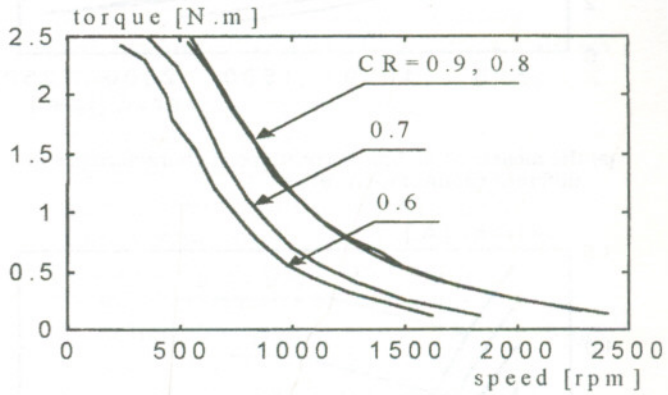

(a) the experimentally measured torque-speed characteristics at different commutation ratios

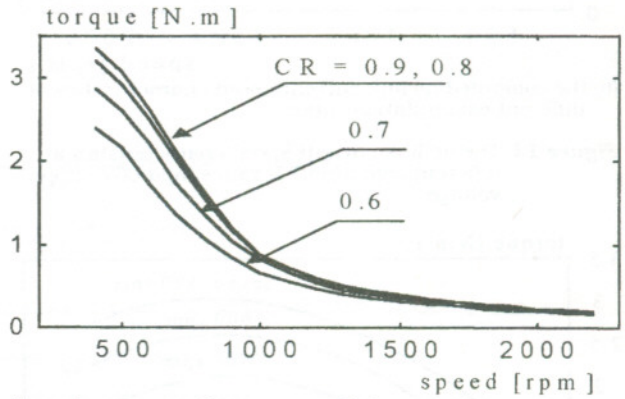

(b) the computed torque-speed characteristics at different commutation ratios

Figure 12 Torque-speed characteristics at different commutation ratios, and 60V supply voltage

From the results shown in Figures 12 and13, it is observed that dc link current and consequently input power have increased by increasing the commutation ratio, as shown in Figure13, However this result is not always valid for the torque curves as shown in Figure 12. where the developed torque is maximum for certain range of commutation ratio.

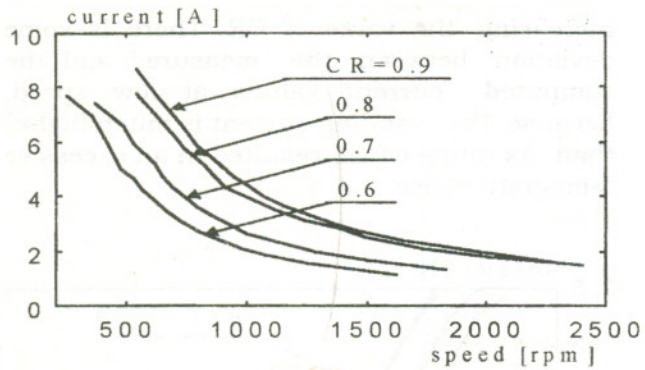

(a) the measured dc link current-speed characteristics at different commutation ratios

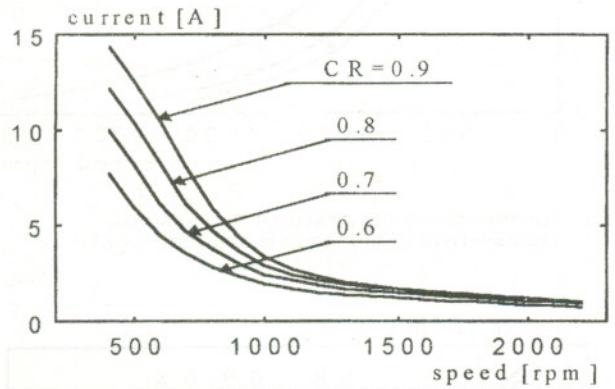

(b) the computed dc link current-speed characteristics at different commutation ratios

Figure 13 The dc link current-speed characteristics at different commutation ratios, and 60V supply voltage

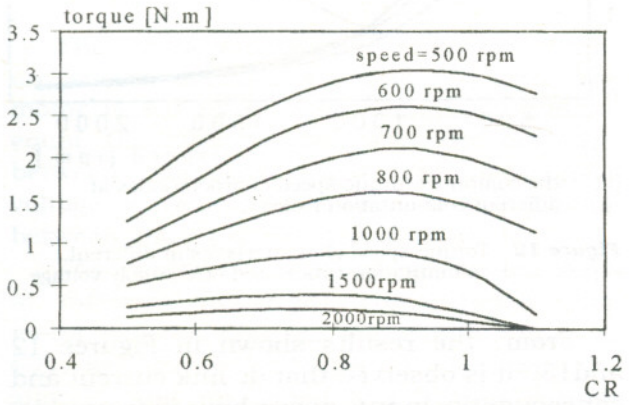

Figure14 Torque against CR at different speeds

The relation between the developed torque and commutation ratio at different speeds has been investigated theoretically and shown in Figure14. It is noticed that the developed torque is maximum for a commutation ratio of certain value between 0.8 and 0.9, however this value tends to be high for low speeds. Up to the peak torque any increase of CR results-in wider current pulses which contribute more positive torque. Any attempt to increase CR after the peak torque results-in some negative torque which will be subtracted from the developed positive torque and the resultant will be lower.

CONCLUSIONS

The proposed four poles per phase SRM has been built, experimentally tested and analytically investigated. Both instantaneous voltage and current waveforms as well as torque-speed and current-speed characteristics have been tested and obtained analytically. An optimum range for commutation ratio has been devised to maximize the developed torque. It has been noticed that the developed torque is maximized for a commutation ratio of a certain value between 0.8 and 0.9, however this value tends to be high for low speeds. In general, simulation and experimental results was found to be in a good agreement. During experimental work it has been noticed that the operation of the proposed motor is extremely quite and smooth. This is due to more distribution of tangential forces and better mapping of flux linkage.

APPENDIX

The motor data

number of stator poles	12
number of rotor poles	8
number of phases	3
the active iron length	40.9 mm
the stator outer diameter	145.5 mm
the stator inner diameter	85.3 mm
stator pole pitch	22.35 mm
apparent stator pole arc	13.8 mm
net stator pole arc	8.4 mm
stator inter polar width	9.45 mm
Rotor diameter	84.8 mm
Rotor pole arc	0.5 rotor pole pitch

REFERENCES

1. J.W.Finch, M.R.Harris, A.Musoke and H.M.B.Metwally, "Variable-Speed Drives Using Multi-Tooth Per Pole Switched Reluctance Motors", 13th International Motion Control System Symposium, University of Illinois, Urbana-Champaign, IL, pp. 293-302. (1994).
2. M.A.El-Khazendar, "The Design of Switched Reluctance Disc Motors Based on Linear Modeling", ICEM Conference, Munchen, pp.1027-1030, (1986).
3. C.Pollock, B.W.Williams, "The Design and Performance of a Multiphase Switched Reluctance Drive", EPE Conference, Aachen, pp. 29-34, (1989).
4. M.M.Khater, A.A.Hassanein, M.M.El-Shanawany, and B.W.Williams, "A five Phase Switched Reluctance Motor Part1: Design and Performance", Engineering Research Bulltin, Menoufya University, Shebin El-Kom, Egypt, Vol. 17, Part1, pp. 121-135, (1994).
5. Stephen Hsien-Yuan Li, Feng Liang, Yifan Zhao and Thomas A. Lipo, "A doubly Salient Doubly Excited Variable Reluctance Motor", IEEE Transactions On Industry Applications, Vol.31, No1, pp. 99-106, (1995)
6. H.C. Lovatt, J.M. Stephenson, "Influence of Number of Poles Per Phase in Switched Reluctance Motors", IEE Proceedings, Part B, Vol.139, No.4, pp. 307-314, (1992).
7. J.Corda and J.M. Stephenson, "Analytical Estimation of The Minimum And Maximum Inductances of A Doubly Salient Motor", Proceedings of Int.Conf on Stepping Motors and Systems, Leeds UK. September pp. 50-59 (1979).
8. M.M.Khater, "Performance and Control of Switched Reluctance Motors", Ph.D thesis, Menoufya University, Shebin El-Kom, Egypt, pp. 81-82. (1994).
9. J. Corda, S. Masic, T. Malijan, E. Skopljak, "Dynamic Performance of Switched Reluctance Motor", Proceedings of ICEM, pp.1023-1026, (1986).
10. T.J.E. Miller, "Converter Volt Ampere Requirements of the Switched Reluctance Motor Drive", IEEE Trans on Industry Applications, Vol. IA-21, No.5,. pp. 1136-1144, (1985).

Received August 16, 1998
Accepted March 16, 1999

أثار نسبة التبديل على خصائص تشغيل محرك الممانعة المتغيرة ثلاثي الأوجه المكون من أربعة أقطاب لكل وجه

محمود أحمد عبد اللطيف ، محمود مصطفى خاطر ، سلوى محمد رياض طاحون ، محمد مصطفى الشنوانى و سيد أحمد حسن

قسم الهندسة الكهربية – جامعة المنوفية

ملخص البحث

يتكون محرك الممانعة المتغيرة التقليدى من أقطاب بارزة في كل من العضوين الثابت والدوار، حيث يزود كل قطبين متقابلين من العضو الثابت بملفات بسيطة متمركزة حول تلك الأقطاب وتوصل هذه الملفات بالتوالى أو التوازى لتشكل أحد أوجه المحرك، وتغذى تلك الملفات من مصدر لنبضات التغذية يتم التحكم فيه تبعا لزاوية وضع أقطاب العضو الدوار، و يتولد العزم في هذا المحرك عن طريق ميل أقطاب الدوار للانحراف لكى تتقابل مع أقطاب الثابت للوجه المغذى، وقد أجمعت الدراسات السابقة التى تمت على هذا الشكل التقليدى للمحرك أنه يعانى من العزم النبضى وارتفاع مستوى الضوضاء الناتجة عنه، وقد ظهرت مؤخرا بعض الدراسات والأبحاث التى تقدم نماذج جديدة للتركيب الداخلى للمحرك لمحاولة تحسين خصائص تشغيله

تقدم هذه المقالة دراسة تحليلية وعملية لأثار نسبة التبديل على خصائص التشغيل لنموذج معدل من محرك الممانعة المتغيرة ثلاثى الأوجه يتركب من عدد أقطاب ٨/١٢ فى الثابت والدوار على التتابع، حيث هذا التركيب يعطى توزيعا أفضل لكل من الفيض